PNAS
www.pnas.org

Supplementary Information for

Rapid evolution of decreased host susceptibility drives a stable relationship between ultra-small parasite TM7x and its bacterial host

Batbileg Bor, Jeffrey S. McLean, Kevin R. Foster, Lujia Cen, Thao T. To, Alejandro Serrato-Guillen, Floyd E. Dewhirst, Wenyuan Shi and Xuesong He

*Correspondence should be addressed to B.B. (bbor@forsyth.org) or X.H. (xhe@forsyth.org)

This PDF file includes:

Supplementary Information

SI Materials and Methods

Since '*Nanosynbacter lyticus*' strain TM7x has been cultivated very recently, many of the assays are newly developed or modified from existing ones. All the assays were tested thoroughly before being applied in our experiments.

Bacterial Strains and Growth Conditions

XH001 (*Actinomyces odontolyticus* subsp. *Actinosynbacter strain XH001*) monoculture and strain TM7x ('*Nanosynbacter lyticus'* Type-Strain TM7x HMT-952) with its host XH001 were previously isolated from the human oral cavity (1). Naïve strain XH001n monoculture was isolated from the same individual independently. All bacterial cultures, including Actinomyces strains from the Forsyth Institute strain collection, were grown in Bacto Brain Heart Infusion (BHI, BD) medium at 37 °C in microaerophilic chamber (2% O_2, 5% CO_2, balanced with N_2). Before each experiment, cells from frozen stock were recovered and passaged twice in BHI to ensure homogeneity (~10-30 µL frozen stock inoculated into 1 mL of BHI and incubated for 24 hours before being re-passaged into 20 mL fresh BHI).

Colony morphology characterization

BHI grown cultures were diluted 10, 10^2, 10^3, 10^4, 10^5, 10^6, 10^7 and 10^8 –fold and 20 µL of diluted cultures was spotted on a blood agar plates (1.5% agar, 5% fresh sheep blood in BHI). Plating was carried out in triplicates for each culture. The plates were dried for 20 minutes at room temperature and subsequently incubated in microaerophilic chamber at 37°C for 3 days. Spots with well separated colonies were imaged under the T-26001 Stereo Microscope (VisionScope2, 10x & 20x, Ken-a-vision), and regular shaped and irregular shaped colonies within the spots were counted.

To determine the presence of TM7x in an individual colony, regular or irregular colonies were directly suspended into PCR mix with TM7x specific 16S primers (2) and subjected to PCR amplification. PCR products were visualized on an agarose gel to determine the presence of a TM7x-specific band (Fig. S1b). We also inoculated individual regular or irregular colonies in 1 mL of BHI and incubated for 24 hours before passaging in fresh media for 5-8 passages. For each passage, culture samples were visualized under the phase-contrast microscope to determine if there were TM7x cells present. Colonies for PCR and cultivation assays were collected from three independent plating experiments (Fig. S1c).

Live imaging of mono and cocultures

Mono- or cocultures were grown in BHI for 10-13 hours in a microaerophilic chamber until log phase. Cultured cells were placed on a 2% agar pads, and these pads were placed on a glass bottom 35 mm petri dish, sandwiching the bacteria between the glass slide and the agar pads. The dishes were incubated in the microaerophilic chamber at 37°C for 1-1.5 hours. All edges were sealed by petroleum jelly. The dishes were removed from the chamber and placed on a heating plate designed to hold 35 mm dishes at 37°C. The images were taken every 5 min for up to 200 min or more using 100x immersion objective with Nikon TE200 microscope.

To analyze the cell growth, we analyzed each movie sequence in FIJI software (3), and cropped target cells with quality resolution to create individual image series. Each image series was converted to binary black and white images with the same threshold applied to all images. Area for each cell was determined by the analysis tool and exported to an excel file. The area increase for each cell was plotted as time vs cell area using KaleidaGraph (Synergy Software). We calculated and plotted the average of all cell areas (Fig. 2a,b). To determine the growth rate, each cell area trace was fitted individually with typical exponential growth equation using KaleidaGraph (Fig. S2a, b):

$$P(t) = A \times e^{kt}$$

From this fit, k (growth rate) was given by m2 constant and summarized in Fig. 2c. P(t) is final cell area at t minutes (or time, x). A is starting cell area (m1). Since we compared each group separately (Fig. 2c), we used the student t-test to determine p values. Growth rate values with data points are shown in a dot plot.

Determining growth rate using OcelloScope, optical cell density measurement

Triplicate wells containing XH001 monoculture or TM7x/XH001 coculture cells were loaded into 96-well plates with starting optical density of 0.025 (250 µL volume). The analogous cell density measurement (TANormalized) was acquired using OcelloScope (BioSense Solutions) every 60 minutes. The exact same method was used to determine the growth curve of naïve XH001n, and regular/irregular colonies (Fig S6d).

To determine the growth rate, the natural log of TANormalized reading was plotted against the time to determine the linear region. Subsequently, the linear region was fitted with linear regression to determine the best fitted line. This fit was used to calculate the growth rate using following equation:

$$k = \frac{\ln(OD2) - \ln(OD1)}{time\ 2 - time\ 1}$$

Isolation and quantification of host-free TM7x

TM7x/XH001 coculture (420 mL) was grown to maximum cell density (see first section). On the day of TM7x isolation, we centrifuged the coculture at 4500 x g for 10 min to pellet the large host cells and attached TM7x. The supernatant was subsequently transferred to new 50 mL tubes. Using 150 mL 0.45 µm Stericups (Millipore, Filtration System), the supernatant containing host-free TM7x cells was filtered using a house vacuum. Filtered samples were transferred to sterilized 6 x 100 mL ultracentrifuge tubes (Quick-Seal, Ultra-Clear, 38 x 102 mm tubes) for a 45 Ti rotor. From here on, all procedures were carried out at 4 °C. Filtered supernatant was centrifuged at 120,000 x g for 90 minutes to pellet the TM7x and resuspended in 1 mL of sterile PBS (Fig. S4). Cells were centrifuged again in table-top centrifuge at 17,000 x g for 20 min at 4 °C. Pelleted TM7x cells were resuspended in 1 mL of sterile PBS and stored on ice until use. We visually confirmed isolated free-floating TM7x cells by phase contrast microscopy (Fig S4a) as well as by PCR using TM7x or XH001 specific primers (Fig. S4b).

Concentration of TM7x cells was determined by a modified version of a previously developed virus counting assay (4). A 220 nm pore size PVDF support filter (Millipore) was first placed onto a fritted glass base. The support filter was then saturated with particle-free water and the 30 nm PCTE filter (SterliTech) was placed on the support filter. Slight vacuum suction was applied to absorb water drops into the membrane with no air bubbles or gaps. The funnel was then mounted on the membrane and the fritted base and clamped down to secure the assembly. 0.5 mL of TM7x (differentially diluted) was added to the funnel and drawn through the 30 nm filter at approximately -70 kPa vacuum. After releasing vacuum, 0.5 mL of a 1:400 diluted (in 10 mM Tris-Base, 1 mM EDTA, pH8.0) SYBR Gold (Invitrogen) solution was added to the funnel to stain TM7x cells for 10 minutes in the dark. Vacuum was applied to draw the SYBR Gold solution and the membrane was washed with 1 mL of 10 mM Tris-Base, 1 mM EDTA, pH 8.0 buffer. We examined staining of both live and fixed TM7x. Fixed TM7x cells displayed large aggregates whereas live cells remained as individual cells. While the filter wash process was underway, a 5 µL drop of 1x SlowFade Gold antifade reagent (Life technologies) was placed on the clean microscope slides, and an additional 5 µL drop was placed on a cover slip. After the filtration, the 30 nm membrane was removed with forceps and waved very gently in the air a few times to dry. The membrane was then placed on the 5 µL of mounting solution on the glass slide facing up and the cover slip was placed on top. Any air bubble was removed and TM7x cells were viewed under

blue excitation (488 nm) using Nikon Eclipse E400 microscope equipped with a Nikon Plan Fluor ×100/1.30 oil immersion objective and epifluorescence capability (Fig. S4c,d). We acquired 40 fields of view per slide and three slides per dilutions. Samples were imaged within a few hours of preparation.

To determine the original concentration of isolated TM7x from the epifluorescence images, we averaged the number of TM7x counted from 40 fields of view, where each field of view had 10685 μm^2 area. We extrapolated the number of TM7x in the original diluents based on the ratio of field of view area to filter area (with a diameter of 15.5 mm). Once we determined the number of TM7x on the filter for each dilution, it was normalized to 0.5 mL (volume that filtered through the membrane) to obtain cells/mL. The determined cells/mL was plotted against the dilution factors from the original sample to create a linear regression (Fig. S4e), which allowed for calculation of the original cell number in the isolated sample.

We also measured the cell density (at 600 nm) of 10^9 TM7x cells/mL to determine TM7x's contribution to OD600 measurement of the coculture. The OD600 value was 0.05±0.03, suggesting that TM7x cell density does not contribute significantly to our measurements.

Re-infection assay with free-floating TM7x

XH001n monoculture grown for two passages (see growth conditions) was aliquoted into fresh tubes (x3) with each tube containing final colony forming units (cfu) of ~$4.5x10^6$. The cells were pelleted by centrifuging at 13,000 x g for 5 minutes and resuspended in 300 µL of fresh BHI. To each tube of XH001n, isolated and quantified TM7x was added in 3:1 ratio (TM7x : XH001n). For the controls, we added PBS alone. The mixed cells were incubated for 10 minutes in room temperature and mixed with additional 2.2 mL of fresh BHI, bringing the final volume to 2.5 mL. This culture was incubated for exactly 24 hours in a microaerophilic chamber at 37°C and passaged into fresh media at a final concentration of OD~0.1 (final volume 2.5 mL). We repeated the passaging thereafter every 24 hours by transferring the culture in fresh medium to a final volume of 2.5 mL with OD~0.1. We chose 24 hours because our growth curve showed that TM7x/XH001 reached stationary phase by this time (Fig. S2c). By performing passaging, we tried to mimic continuous culture as much as possible and ensure that nutrient is not a limiting factor for XH001n growth.

During every passage, the optical (cell) density was monitored at 600 nm (OD600) using a Spectronic Genesys 5 spectrophotometer. TM7x score was assigned by observing the cultures under a phase-contrast microscope using 100x immersion objective with a Nikon Eclipse E400 microscope, and assessing the amount of TM7x cells (see Fig. S5a). We want to point out that TM7x scoring is a more qualitative assessment of TM7x than a quantitative measurement. To score the TM7x, we spotted 1 µL culture to glass slides and placed a cover slip on top. We usually observed ~100 cells per viewing field. When one or two XH001n cells were associated with TM7x in a single viewing field, we scored 0.2 (Figure S5a). We visualized at least 5 image fields per sample. When more than two XH001n cells with multiple TM7x appeared on the same cell, we scored 0.5. When many TM7x decorated the same XH001n cell and the majority of the XH001n cells were decorated with TM7x, we scored 0.7. We observed a low level of free-floating TM7x at score 0.7 as well. Lastly, in addition to all conditions met by a score 0.7, if we observed many free-floating TM7x, we scored 1. Live/dead staining was carried out according to the manufacturer's guidelines (Life Technologies) and visualized by using a Zeiss LSM880 confocal microscope.

The total cfu/mL and irregular colony percentage were quantified by plating the cocultures on a blood agar plate and counting the colonies after 2-3 days. We plated the cultures in triplicate and reported the standard deviation as an error bar on the graphs. Regular and irregular colonies were counted separately and total cfu/mL was determined by adding the counts for both types.

To determine the TM7x:XH001n ratio in the re-infection assay, genomic DNA was isolated from each passage of the re-infection assay according to our previous methods (2). For each

sample, we determined the qPCR Ct value using either XH001n or TM7x qPCR specific primers, and the ratio was calculated according to our previous method (2). When host cells become filamentous, such as what we see with XH001, some individual cells may have multiple copies of the genome. Although this was not observed in our DNA staining (2), if this is the case then our qPCR method will overestimate the number of XH001n cells. Even with this bias, however, our key conclusions from the qPCR method will be only reinforced.

Whole-genome sequencing and variant analysis

Three independent naïve XH001n cells were cultured for two passages in BHI, and genomic DNA was isolated for all three samples. We also took the same three naïve cultures and carried out the re-infection experiment with freshly isolated TM7x. The cocultures were passaged six times, and the genomic DNA was isolated for genome sequencing. All three cultures showed population crash at passage 3 and recovered by passage 6. Cells from passage 6 were harvested and DNA extracted for re-sequencing.

Genomic sequencing was performed as previously described (5). Briefly, libraries were prepared using the Nextera XT kit (Illumina, San Diego, CA, USA), according to the manufacturer's specifications. Sequencing was then performed on an Illumina MiSeq platform (2 x 300 bp). The BBDuk [1] tool for Geneious (v 9.1.8) was used to quality trim and filter Illumina adapters, artifacts, and phiX from reads (7). We discarded paired reads with quality scores averaging less than 6 before trimming or with a length under 20 bp after trimming. Remaining reads were mapped using Geneious mapper to the reference XH001n genome (5). We do want to point out that when the XH001n was initially isolated as a monoculture, we did not differentiate it with XH001 (the one associated with TM7x), due to the fact that they were isolated from the same subject and shared identical 16s genes. Therefore, our previously published genome was called XH001 (5), but we now know it is genomically and phenotypically different from XH001. Therefore, in our current study we renamed the strain to XH001n. Polymorphisms were then identified from the comparison using a minimum variant frequency of 0.25 and minimum coverage of 10 reads relative to the reference. Polymorphism frequencies in each culture was determined and gated at >10% threshold. We summarized the data in Table S1. We only summarized unique mutations (compare to naïve XH001) found in all three replicates cultures recovered from crash at passage 6. We predicted that mutations that occur in all three replicates with 10% or higher variant frequency would have a higher chance of contributing to the resistant phenotype we observed.

Pan-genome analysis

The available genomes of *Actinomyces* strains in Figure S7a were acquired from the Human Oral Microbiome Database (HOMD) (6). Subsequently, we tested genome completeness by the presence and absence of specific marker genes using CheckM (7). All genomic sequences were re-annotated to use the same gene prediction algorithm. Open reading frames and annotations were performed using Prokka (8). The comparative genomic analysis was executed using Roary, which clusters proteins using MCL-edge (9) at 70% amino acid identity cutoff.

Statistical analysis

We included the description of statistical analysis for each experiment and procedure as necessary (see above sections). Where appropriate, we used a dot plot in combination with box plot to show the actual data. For many of the single cell imaging datasets, we reported total number of cells analyzed from 6 or more independent experiments, rather than individually analyzing each experiment and reporting p value. We believe this is a more accurate comparison since each independent imaging contained a varying number of cells.

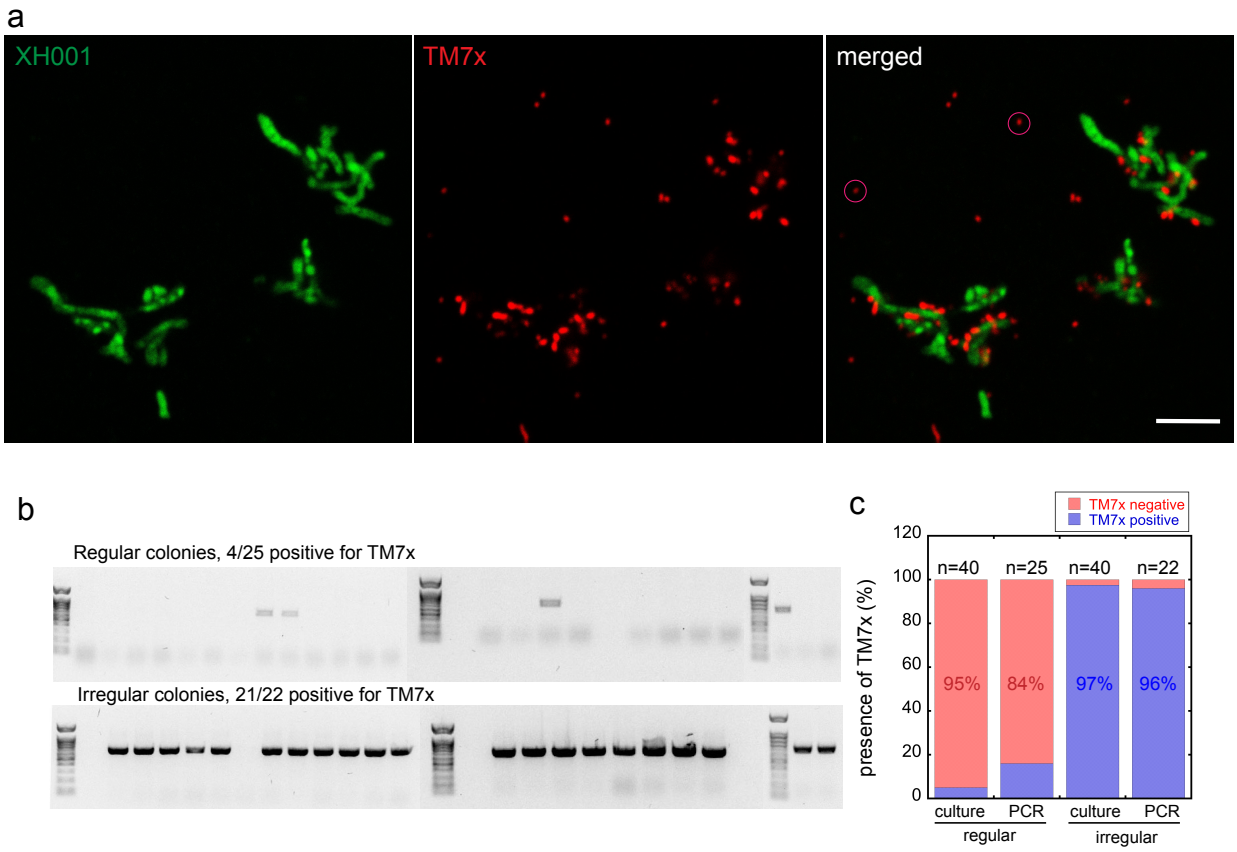

Figure S1. Characterization of established TM7x/XH001 coculture. (a) Fluorescence *In Situ* Hybridization (FISH) imaging of TM7x (red) and XH001 (green) using 16S DNA probes specific to Saccharibacteria and *Actinomyces odontolyticus* as in our previous work (2). In the merged image, red circles are indicating free-floating TM7x that stained with the Saccharibacteria specific probes. Scale bar: 5 µm. (b) PCR test of TM7x presence in the regular (n=25) and irregular (n=22) colonies. Although, four regular colonies tested positive for TM7x, they all showed very faint band compare to irregular colonies, suggesting that these regular colonies tested positive because they might have been contaminated while we were picking the colonies. The final quantification is shown in c. (c) Regular and irregular colonies from the coculture were grown several passages (culture) or directly lysed for colony PCR to detect TM7x. The stacked bar graph reflects the presence (blue) or absence (red) of TM7x in each colony (see b for PCR results).

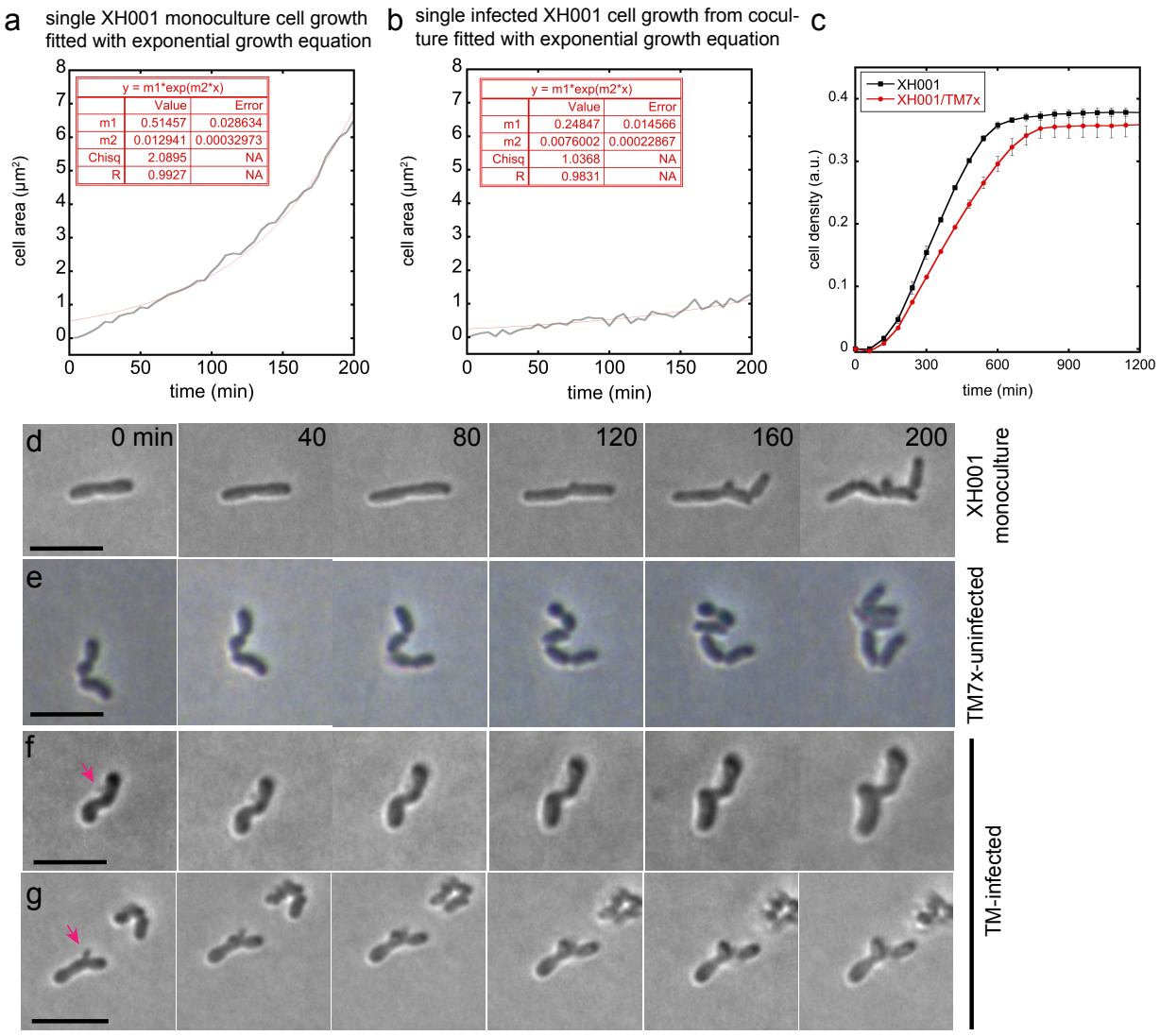

Figure S2. Live imaging of TM7x-uninfected and -infected XH001. Representative graph showing XH001 monoculture cell (a) or TM7x-infected XH001 cell from coculture (b) that were individually tracked for their cell area growth. These traces were fitted with exponential growth equation (red, see methods) to determine the growth rate (min^{-1}). Red box containing m1 (starting cell area) and m2 (growth rate) constants, as well as the R (goodness of fit) were generated from the fit (see methods). The growth rates were determined this way for each cells in Figure 2a and 2b, and summarized in Fig. 2c. (c) The bulk growth of mono and cocultures were determined using an OcelloScope, which is an image based cell density measurement (see methods). The growth rates were calculated from the linear regression analysis that was fitted to the exponential growth phase of the curves. (d) Few cells in the XH001 monoculture grew by segmentation where cells grew to long filaments before segmenting into smaller cells. (e) TM7x-uninfected XH001 cells in coculture grew similar to XH001 monoculture cells with no difference in growth rate. Many TM7x-infected host cells grew without cell division (f) or grew branches (g). These modes of growth were rarely seen in monoculture. Scale bars: 5 μm. Arrows indicate TM7x.

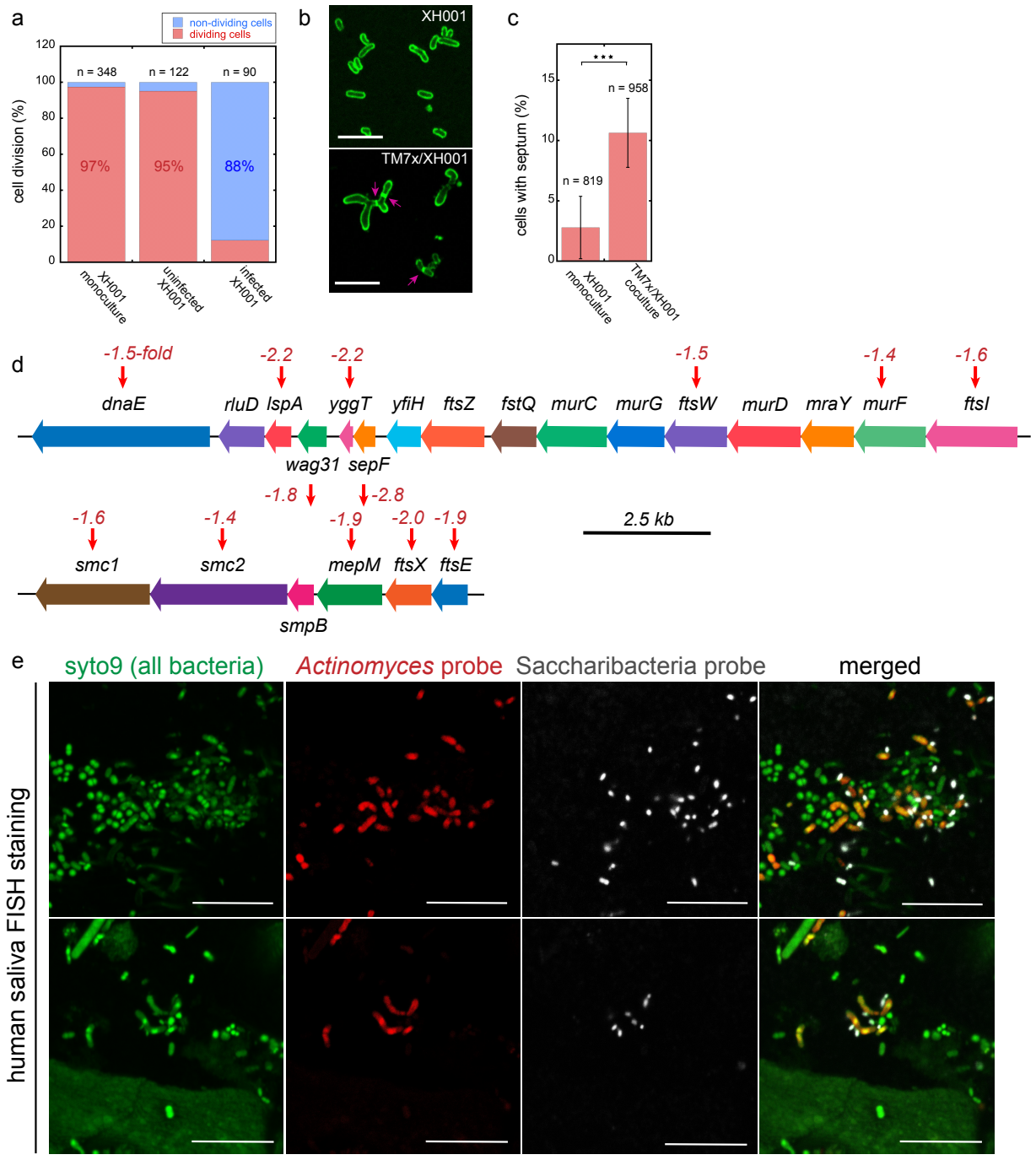

Figure S3. Host cell division is severely inhibited. (a) Portion of cells that divided (one or more time) during the single cell imaging. n reflects total number of cells tracked from at list 6 independent experiments. (b) XH001 cell membrane staining (WGA-Alex488) of mono or cocultures reflect increased septum (arrows) in cells from coculture. Coculture cells also displayed uneven staining of the membrane. Scale bars: 5 μm. (c) The number of cells containing cell septum from panel b was enumerated. n reflects total number of cells counted from three independent experiments. *** denote p value of <0.0001. (d) Cell division gene cluster regions

reflect the significantly down-regulated mRNA levels (red-down arrow) by transcriptomics in mono vs coculture cells. The data was acquired from our previous publication (1). (e) Saccharibacteria sparsely infects host *Actinomyces in vivo*. FISH imaging of human saliva bacteria using Saccharibacteria or *Actinomyces* specific probes showed that only a few Saccharibacteria cells decorate individual *Actinomyces* host cells. Scale bars: 10 μm.

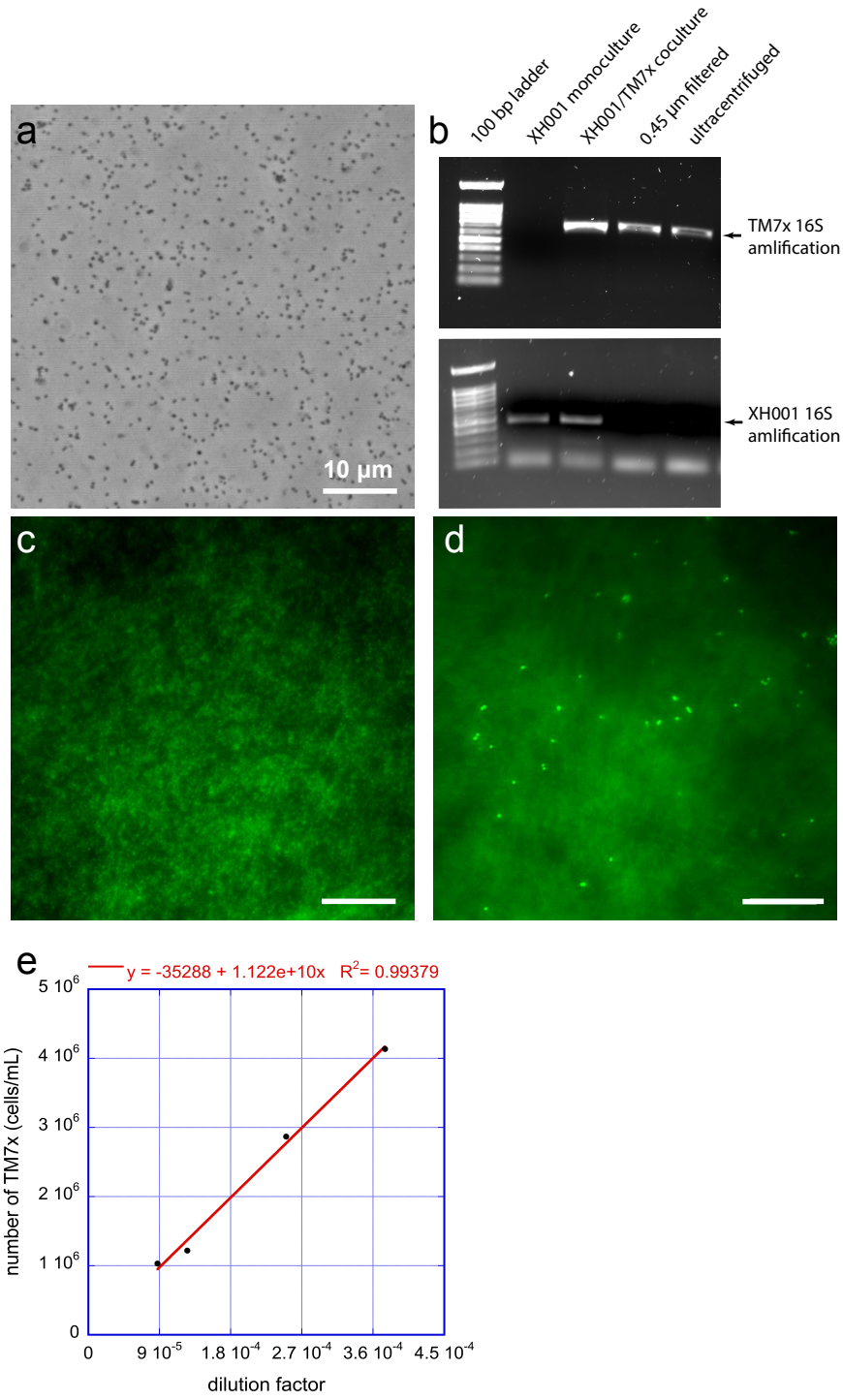

Figure S4. Isolation of free-floating TM7x. (a) Using our current TM7x isolation method (see methods), we acquired high number of TM7x that can be easily seen under the phase-contrast microscope. (b) Using species-specific 16S primers, we amplified TM7x or XH001 specific PCR products from the genomic DNA purified from the isolated TM7x as well as XH001 mono and TM7x/XH001 cocultures at each stage of purification. (c) Fluorescently labeled 30 nm PCTE filter membrane visualized by the epifluorescent microscope. (d) Fluorescently labeled 30 nm PCTE

filter membrane that has TM7x cells attached. See methods for staining procedure. Scale bars: 5 μm (c and d). (e) The standard curve of original dilution (isolated TM7x) vs. the numerated TM7x from the membrane (see methods) using virus counting method. We fit the data with linear regression and the slope of the fit (1.12×10^{10}) indicates the number of TM7x cells/mL in the original sample. We conducted multiple experiments and only the representative result is shown.

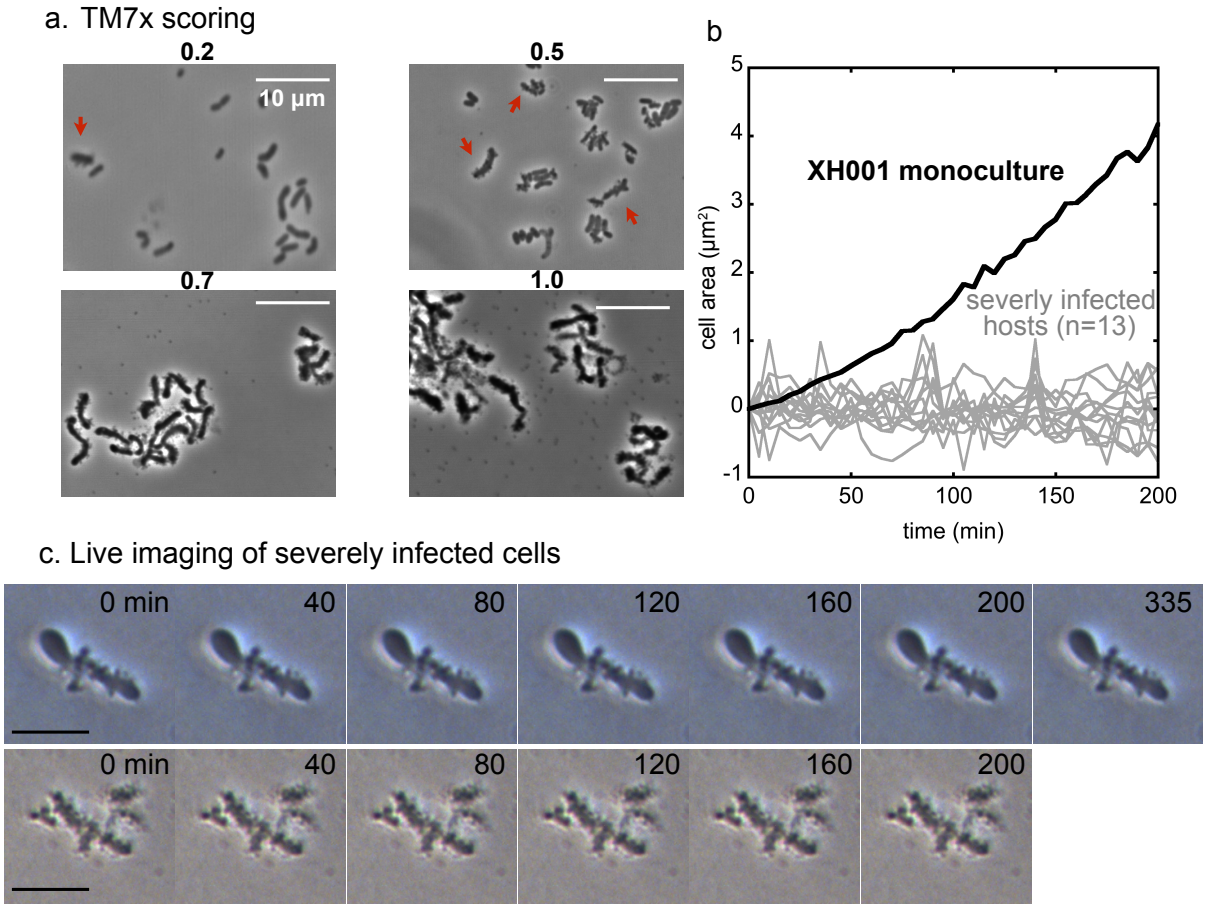

Figure S5. TM7x scoring method and live imaging of severely infected host cells. (a) Using a phase contrast microscope, we visualized the TM7x in re-infection assay at every passage, and scored them according to the amount of TM7x we observed under the microscope. When the XH001n showed no TM7x, the score was 0 and the highest amount of TM7x seen in the cultures received a score of 1. See method section for detailed scoring criteria. Scale bar: 10 µm. Red arrows are indicating infected hosts. (b) We tracked the cell growth of 13 severely infected XH001n cells and none of them showed any growth compared to XH001 monoculture cells. (c) During crash phase of growth, the severely infected XH001n cells were live imaged (see methods). All host cells did not show growth or lysis after 335 minutes. Scale bars: 5 µm.

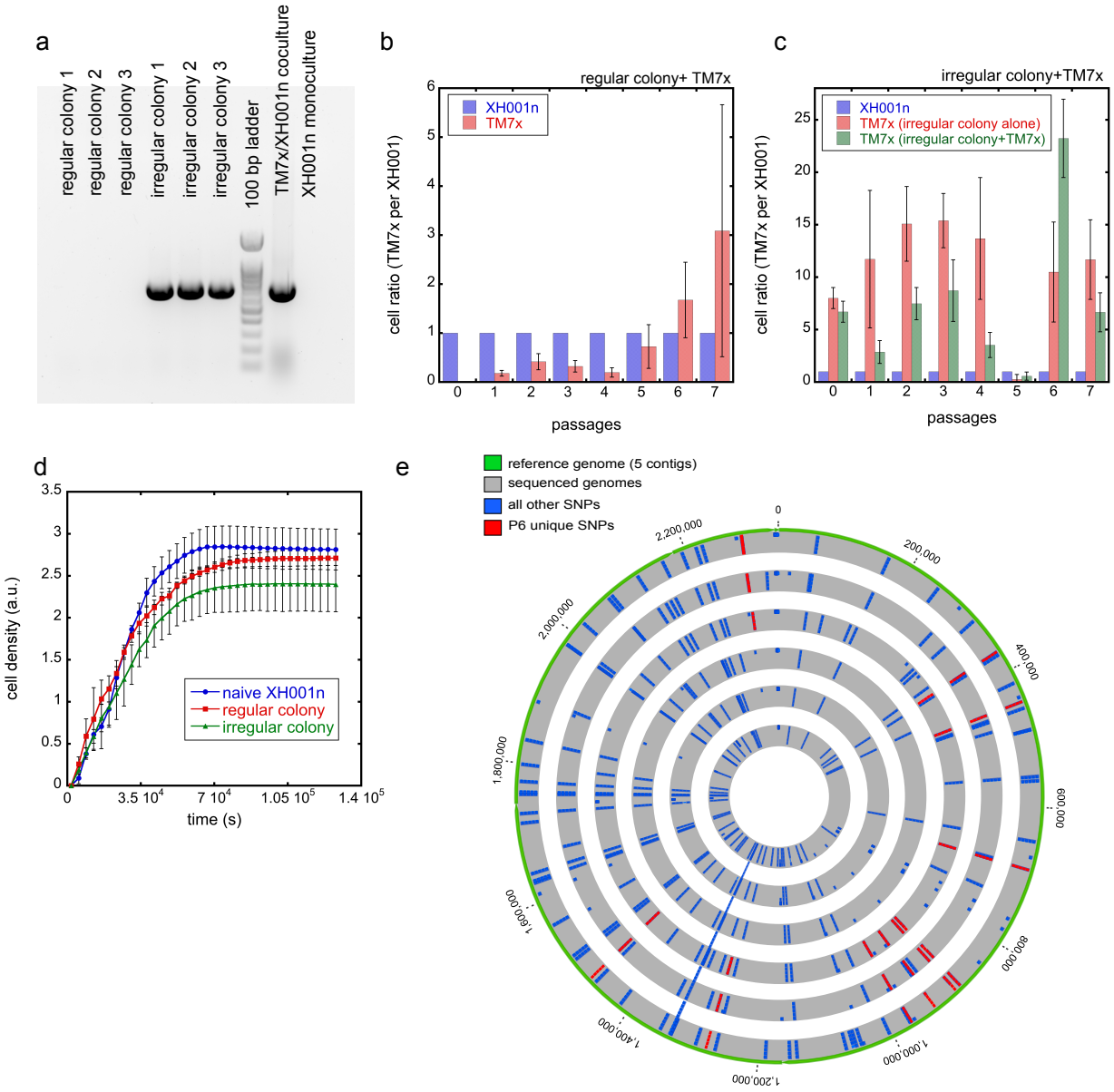

Figure S6. Host evolves reduced-susceptibility to TM7x. A re-infection assay was carried out and cells were harvested at passage 6, the culture that was recovered from the growth crash was plated on agar plates. From this, we recovered three regular and three irregular colonies and they were tested for presence of TM7x using PCR (a). The growth profile of these six colonies were determined by OcelloScope (d, see methods) and showed very similar pattern to already established mono and cocultures. The cultures derived from irregular colonies showed slightly slower growth than those from regular colonies. We also recovered regular colonies from naïve XH001n culture, which was used as a control for Fig. 4a-c. The TM7x to XH001n ratio was determined by qPCR for the experiments show in Fig 4a and b (b and c). (e) Circular map of three re-sequenced genomes of naïve XH001n (inner circles) cultures and three genomes of TM7x/XH001n cocultures (outer circles) recovered from TM7x-induced growth crash (passage 6). Blue lines indicate the position of each Single Nucleotide Polymorphism compared to the

reference naïve XH001n genome. Red lines indicate the 10 mutated genomic positions unique to all three XH001n hosts that have reduced-susceptibility. These ten genes are summarized in Table S1.

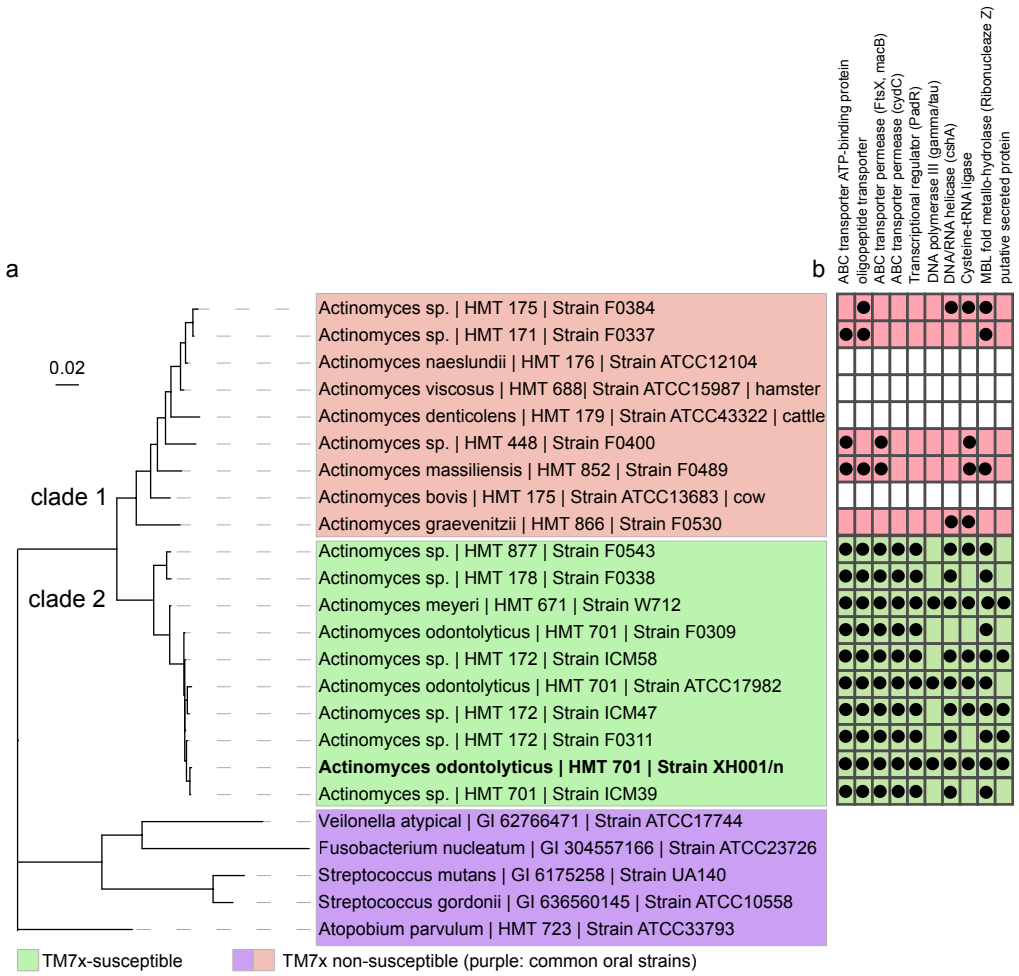

Figure S7. Genes with variants in XH001n that may confer reduced-susceptibility to TM7x infection were predominately found in clade 2. (a) Different *Actinomyces* (red, green) and common oral bacterial (blue) species were tested in re-infection assay. A phylogenetic tree was created using the 16S sequences of these species. The screen revealed that TM7x was able to infect only *Actinomyces* species from clade 2 (green) that are closely related to XH001n (bolded), but not able to infect *Actinomyces* species from clade 1 (red) or other oral bacterial strains (blue). (b) Pan-genome analysis was carried out using 15 available genomes from the HOMD database for *Actinomyces* strains in a. Strains with no available genomes are shown in white blank rows. Green-clade 2 is TM7x growth supporting strains while red-clade 1 is non-supporting strains. Ten genes from Table S1 are listed on the top and the presence of each gene (or their homologues) is indicated by black dot. The homology cut of was performed at 70% (see methods section).

Table S1. Observed mutations in XH001n when passaged with TM7x.

Protein identification	Track Name (Replicates)	Genome position	NCBI locus tag	Amino Acid Change	Nucleotide Change	Codon Change	Polymorphism Type	Protein Effect	Variant Frequency	Variant P-Value (approximate)	Total length (aa)	mut position (aa)	Predicted domains (phyra 2)
ABC transporter ATP-binding protein*	1_P6_TM7x-XH001	692,667	KSW13310.1	M -> V	T -> C	ATG -> GTG	SNP (transition)	Substitution	47.90%	1.50E-126	266	196	2-266
	2_P6_TM7x-XH001	692,667	KSW13310.1	M -> V	T -> C	ATG -> GTG	SNP (transition)	Substitution	40.30%	1.50E-135			
	3_P6_TM7x-XH001	692,667	KSW13310.1	M -> V	T -> C	ATG -> GTG	SNP (transition)	Substitution	11.60%	2.40E-25			
oligopeptide transporter*	1_P6_TM7x-XH001	885,049	KSW13460.1				Deletion	Frame Shift	35.80%	2.10E-30	666	28	316-666, 2-15, 8-184
	2_P6_TM7x-XH001	885,049	KSW13460.1				Deletion	Frame Shift	45.90%	9.40E-73			
	3_P6_TM7x-XH001	885,049	KSW13460.1				Deletion	Frame Shift	16.70%	2.10E-15			
ABC transporter permease (FtsX, macB 4)*	1_P6_TM7x-XH001	972,678	KSW13518.1	G -> D	G -> A	GGT -> GAT	SNP (transition)	Substitution	37.50%	9.70E-58	421	356	1-419, 43-289, 296-364
	2_P6_TM7x-XH001	972,678	KSW13518.1	G -> D	G -> A	GGT -> GAT	SNP (transition)	Substitution	37.10%	1.30E-78			
	3_P6_TM7x-XH001	972,678	KSW13518.1	G -> D	G -> A	GGT -> GAT	SNP (transition)	Substitution	30.30%	4.00E-48			
ABC transporter permease (CydC)*	1_P6_TM7x-XH001	1,471,439	KSW11046.1	Q -> H	G -> C	CAG -> CAC	SNP (transversion)	Substitution	44.20%	4.40E-62	533	185	2-533, 2-302
	2_P6_TM7x-XH001	1,471,439	KSW11046.1	Q -> H	G -> C	CAG -> CAC	SNP (transversion)	Substitution	34.40%	4.00E-85			
	3_P6_TM7x-XH001	1,471,439	KSW11046.1	Q -> H	G -> C	CAG -> CAC	SNP (transversion)	Substitution	11.80%	5.60E-22			
Transcriptional regulator, PadR family*	1_P6_TM7x-XH001	369,671	KSW13085.1	Q -> H	C -> A	CAG -> CAT	SNP (transversion)	Substitution	11.20%	7.30E-29	202	39	1-166, 2-85
	2_P6_TM7x-XH001	369,671	KSW13085.1	Q -> H	C -> A	CAG -> CAT	SNP (transversion)	Substitution	38.10%	2.70E-144			
	3_P6_TM7x-XH001	369,671	KSW13085.1	Q -> H	C -> A	CAG -> CAT	SNP (transversion)	Substitution	24.80%	1.20E-64			
DNA polymerase III subunits gamma and tau#	1_P6_TM7x-XH001	448,514	KSW13147.1	T -> N	G -> T	ACC -> AAC	SNP (transversion)	Substitution	47.40%	1.30E-49	985	600	2-373,
	2_P6_TM7x-XH001	448,514	KSW13147.1	T -> N	G -> T	ACC -> AAC	SNP (transversion)	Substitution	29.30%	7.70E-27			
	3_P6_TM7x-XH001	448,514	KSW13147.1	T -> N	G -> T	ACC -> AAC	SNP (transversion)	Substitution	29.80%	3.90E-29			
putative ATP-dependent RNA helicase, cshA#	1_P6_TM7x-XH001	1,277,641	KSW10891.1	Q -> E	G -> C	CAG -> GAG	SNP (transversion)	Substitution	54.80%	2.80E-67	588	184	67-445,
	2_P6_TM7x-XH001	1,277,641	KSW10891.1	Q -> E	G -> C	CAG -> GAG	SNP (transversion)	Substitution	29.80%	5.30E-34			
	3_P6_TM7x-XH001	1,277,641	KSW10891.1	Q -> E	G -> C	CAG -> GAG	SNP (transversion)	Substitution	17.90%	5.70E-24			
cysteine--tRNA ligase^	1_P6_TM7x-XH001	931,549	KSW13495.1	L -> F	C -> T	CTC -> TTC	SNP (transition)	Substitution	33.30%	9.90E-47	485	128	1-484

	2_P6_TM7x-XH001	931,549	KSW13495.1	L -> F	C -> T	CTC -> TTC	SNP (transition)	Substitution	32.10%	1.60E-55			
	3_P6_TM7x-XH001	931,549	KSW13495.1	L -> F	C -> T	CTC -> TTC	SNP (transition)	Substitution	12.10%	1.40E-16			
Ribonuclease Z, MBL fold metallo-hydrolase^	1_P6_TM7x-XH001	2,283,473	KSW10286.1	D -> G	A -> G	GAC -> GGC	SNP (transition)	Substitution	42.50%	1.90E-82	265	208	1-265, 190-262
	2_P6_TM7x-XH001	2,283,473	KSW10286.1	D -> G	A -> G	GAC -> GGC	SNP (transition)	Substitution	42.70%	9.60E-134			
	3_P6_TM7x-XH001	2,283,473	KSW10286.1	D -> G	A -> G	GAC -> GGC	SNP (transition)	Substitution	23.90%	1.40E-39			
putative secreted protein	1_P6_TM7x-XH001	893,431	KSW13464.1	Q -> L	A -> T	CAG -> CTG	SNP (transversion)	Substitution	51.50%	1.70E-97	819	482	164-307, 754-804
	2_P6_TM7x-XH001	893,431	KSW13464.1	Q -> L	A -> T	CAG -> CTG	SNP (transversion)	Substitution	50.00%	2.50E-133			
	3_P6_TM7x-XH001	893,431	KSW13464.1	Q -> L	A -> T	CAG -> CTG	SNP (transversion)	Substitution	13.80%	3.00E-17			

*Transporters or transport regulators.
#DNA replication genes during cell division.
^tRNA function or synthesis.

SI Reference

1. He X, et al. (2015) Cultivation of a human-associated TM7 phylotype reveals a reduced genome and epibiotic parasitic lifestyle. *Proc Natl Acad Sci U S A* 112(1):244–249.

2. Bor B, et al. (2016) Phenotypic and Physiological Characterization of the Epibiotic Interaction Between TM7x and Its Basibiont Actinomyces. *Microb Ecol* 71(1):243–255.

3. Schindelin J, et al. (2012) Fiji: an open-source platform for biological-image analysis. *Nat Methods* 9(7):676–682.

4. Diemer GS, Kyle JE, Stedman KM (2012) Counting viruses using polycarbonate Track Etch membrane filters as an alternative to Anodisc membrane filters. Available at: http://web.pdx.edu/~kstedman/.

5. McLean JS, et al. (2016) Draft Genome Sequence of *Actinomyces odontolyticus* subsp. *actinosynbacter* Strain XH001, the Basibiont of an Oral TM7 Epibiont. *Genome Announc* 4(1):e01685-15.

6. Chen T, et al. (2010) The Human Oral Microbiome Database: a web accessible resource for investigating oral microbe taxonomic and genomic information. *Database* 2010(0):baq013–baq013.

7. Parks DH, Imelfort M, Skennerton CT, Hugenholtz P, Tyson GW (2015) CheckM: assessing the quality of microbial genomes recovered from isolates, single cells, and metagenomes. *Genome Res* 25(7):1043–1055.

8. Seemann T (2014) Prokka: rapid prokaryotic genome annotation. *Bioinformatics* 30(14):2068–2069.

9. Page AJ, et al. (2015) Roary: rapid large-scale prokaryote pan genome analysis. *Bioinformatics* 31(22):3691–3693.